ACCSCIENCE PUBLISHING

Tumor Discovery

ORIGINAL RESEARCH ARTICLE

The role of disulfidptosis-related genes in the clinical prognosis and immune status of hepatocellular carcinoma

Qiang Li[1], Yang Li[1], Jiaqian Mo[1], Xin Xie[2], Moxian Chen[3], and Shanshan Wang[1]*

[1]Laboratory of Immunoinflammatory, School of Life Sciences and Biopharmaceutics, Guangdong Pharmaceutical University, Guangzhou, Guangdong, China

[2]School of Life and Environmental Sciences, Shaoxing University, Shaoxing, Zhejiang, China

[3]State Key Laboratory of Tree Genetics and Breeding, Co-Innovation Center for Sustainable Forestry in Southern China, College of Life Sciences, Nanjing Forestry University, Nanjing, Jiangsu, China

Abstract

Drug resistance and poor prognosis in hepatocellular carcinoma (HCC) underscore the urgent need for novel treatments. Disulfidptosis, a recently identified form of metabolism-related regulated cell death, plays a complex role in anti-tumor immunity; however, its precise function in HCC remains unclear. Understanding the proteins and pathways involved in disulfidptosis and its association with disulfidptosis-related genes (DRGs) in HCC could reveal innovative therapeutic strategies. This study employs bioinformatics to examine the correlation between DRGs and both clinical prognosis and immune status in HCC patients. Risk models were constructed using univariate Cox and least absolute shrinkage and selection operator regression to identify significant genes, with risk scores correlated to survival outcomes across various patient subtypes. In addition, the analysis explored the association of DRGs with prognosis, immune cell infiltration, enriched functional pathways, and immune checkpoints. The risk model identified six key genes: *FLNA*, *NCKAP1*, *CD2AP*, *RPN1*, *SLC7A11*, and *CAPKAP*. Validation through the receiver operating characteristic curve demonstrated the model's exceptional predictive power. Gene network analysis revealed ten essential genes, three of which (*FLNA*, *CD2AP*, and *CAPZB*) were shared with the risk model. *FLNA* and *CAPZB* have previously been linked to therapeutic indicators and pathways in HCC. However, there is a lack of comprehensive data connecting *CD2AP* to clinical therapy or HCC pathways. These findings highlight the significance of DRGs in HCC prognosis and immune regulation, suggesting that DRG-targeted therapies may offer new avenues for HCC treatment.

Keywords: *CD2AP*; Disulfidptosis; Hepatocellular carcinoma

***Corresponding author:**
Shanshan Wang
(Bio33@gdpu.edu.cn)

Citation: Li Q, Li Y, Mo J, Xie X, Chen M, Wang S. The role of disulfidptosis-related genes in the clinical prognosis and immune status of hepatocellular carcinoma. *Tumor Discov*. 2025;4(2):66-81. doi: 10.36922/td.8214

Received: December 26, 2024

1st revised: March 17, 2025

2nd revised: March 22, 2025

Accepted: March 26, 2025

Published online: May 19, 2025

Copyright: © 2025 Author(s). This is an Open-Access article distributed under the terms of the Creative Commons Attribution License, permitting distribution, and reproduction in any medium, provided the original work is properly cited.

Publisher's Note: AccScience Publishing remains neutral with regard to jurisdictional claims in published maps and institutional affiliations.

1. Introduction

Hepatocellular carcinoma (HCC) is a prevalent malignant neoplasm of the digestive system and is the most common primary liver tumor. HCC ranks sixth (4.3%) among newly diagnosed cancer cases globally and is the third (7.8%) leading cause of cancer-related deaths worldwide.[1] The annual incidence of HCC has been rising, and the

outcomes of treatment remain suboptimal, with only 15% of patients surviving for 5 years.[2] In China, liver cancer is the third most common cancer and the second leading cause of cancer-related mortality.[3] Most patients succumb to tumor progression and recurrence despite receiving aggressive treatment modalities such as chemotherapy and surgical resection.[4,5] Nevertheless, research suggests that immune checkpoint inhibitor (ICI) therapy offers novel therapeutic options for HCC by targeting various cancers.[6,7] However, studies have not identified any prognostic biomarkers for ICI therapy. Consequently, identifying reliable biomarkers for ICIs in HCC remains of utmost importance.

Disulfidptosis, a recently described form of metabolism-associated regulated cell death, was identified in February 2023 in a study by Liu *et al.*[8] It is associated with disulfide linkages between internal and external protein molecules. Disulfide stress, caused by the accumulation of disulfide-bonded substances in cancer cells with elevated *SLC7A11* expression and glucose deprivation, disrupts the normal binding of disulfide bonds between cytoskeletal proteins. This disruption induces conformational and functional alterations in proteins, ultimately leading to cell death.[8] Research has revealed that the *SLC7A11* gene plays a significant role in disulfidptosis, primarily influencing the development of specific malignancies and anti-tumor immunity. Disulfidptosis is anticipated as a potential cancer treatment, given that previous research has demonstrated the widespread expression of the *SLC7A11* gene in numerous cancer cells.[9] Disulfidptosis-related genes (DRGs) have been used to screen for prognostic markers and potential therapeutic targets in various malignancies, such as colorectal adenocarcinoma.[10] In addition, DRGs have been associated with the development of HCC.[11] Furthermore, numerous studies have demonstrated that *SLC7A11* is associated with cell death across various organs and tissues in the human body. For example, tumor growth has been promoted by the overexpression of *SLC7A11*, partly due to the suppression of ferroptosis, while inhibition of *SLC7A11* is more likely to induce autophagic death and apoptosis as a result of elevated intracellular reactive oxygen species levels.[12] The downregulation of *SLC7A11* has been shown to impair the cysteine metabolic pathway, affecting glutathione synthesis, which leads to the accumulation of lipid peroxides and ultimately causes ferroptosis cell death.[13]

Elevated *SLC7A11* expression has been found to activate the phosphatidylinositol 3-kinase/protein kinase B (PI3K/Akt) pathway, promoting the migration and invasion of pancreatic cancer cells.[14] Moreover, the mechanisms of disulfidptosis have been proposed as a critical new approach to disease treatment.[15] For example, intracellular disulfidptosis has been associated with oxidative stress, and the formation of invasive pseudopods in metastatic tumors has been suggested to exacerbate disulfide bonding stress.[16] Disulfide production is regulated by several signaling pathways, including the nuclear factor kappa B and c-Jun N-terminal kinase pathways.[17] In cardiovascular diseases, cellular damage has been mitigated by inhibiting sulfur dioxide.[18] Thus, disulfidptosis is considered to hold significant potential as a therapeutic strategy. However, the role of disulfidptosis in HCC remains unclear. Hence, in this study, DRGs were identified to develop a risk score model. Genes associated with DRGs were screened using univariate Cox regression and least absolute shrinkage and selection operator (LASSO) regression analyses. A risk model was developed, and its predictive ability was assessed. The association between prognostic and clinical features was examined, followed by functional enrichment analysis and the construction of a protein-protein interaction (PPI) network. Gene set enrichment analysis (GSEA) and immune infiltration correlation analyses were performed to investigate the expression levels of immune checkpoint genes and DRGs in HCC and normal tissues. In addition, the gene expression and drug sensitivity profiles of DRG-related genes in tumors were analyzed. These signaling pathway genes have potential as therapeutic targets due to their roles as oncogenes. To elucidate the role of disulfidptosis in HCC, our study aims to explore the association between DRGs and both the immunological profiles and clinical prognosis of HCC patients.

2. Data and methods

2.1. Materials and data

2.1.1. Data collection

Clinical data for 424 patients with HCC were obtained from the Cancer Genome Atlas (TCGA) database (https://portal.gdc.cancer.gov/). Data from the 424 TCGA-liver HCC samples were standardized using the "Surrogate Variable Analysis" package in R software (version R 4.4.2). Subsequently, 79 immune checkpoint-associated genes were identified from the review,[19] along with 23 differentially regulated genes (*SLC7A11*, *ACTN4*, *GYS1*, *MYH10*, *NDUFS1*, *IQGAP1*, *MYL6*, *NDUFA11*, *PDLIM1*, *NUBPL*, *NCKAP1*, *CD2AP*, *LRPPRC*, *INF2*, *SLC3A2*, *MYH9*, *RPN1*, *ACTB*, *CAPZB*, *DSTN*, *FLNA*, *FLNB*, and *TLN1*) reported by Liu *et al.*[8] The mRNA expression data were normalized using the appropriate R package. A total of 23 genes were selected based on the criteria of |logFC| > 0.5 and false discovery rate (FDR)< 0.05. Differentially expressed genes were initially identified using the "limma" package in R software, identifying 18 DRGs (Figure 1).

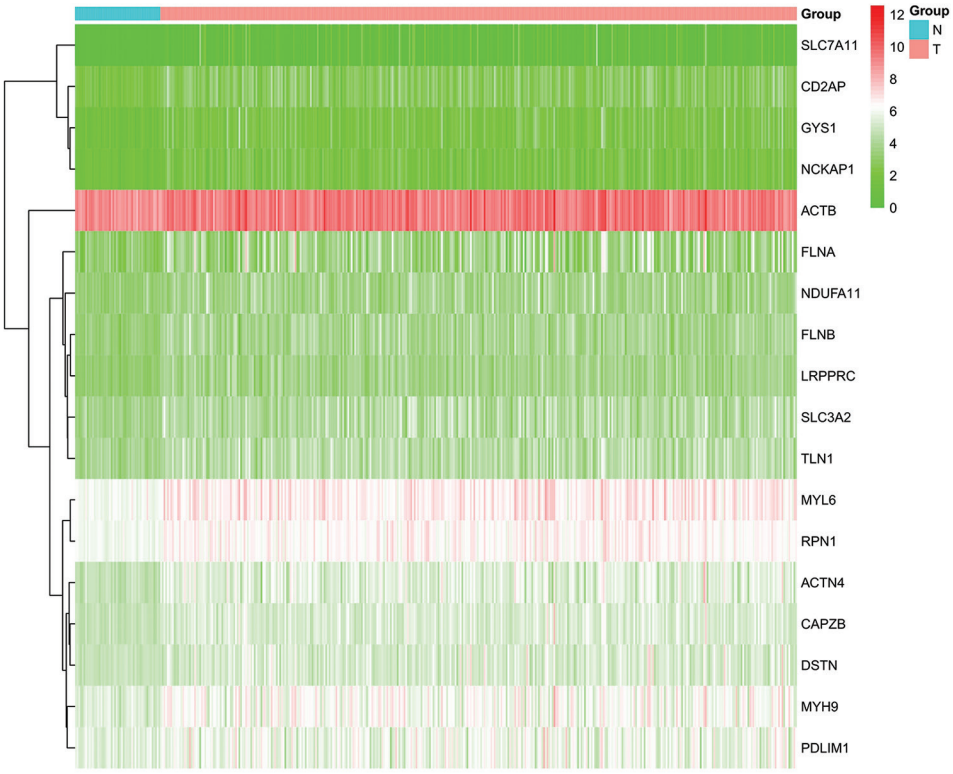


Figure 1. Heatmaps of 18 disulfidptosis-related gene expression levels. Each column represents a sample, and each row represents a gene. N refers to normal tissue, T refers to tumor tissue, red indicates high expression, and green indicates low expression.

2.1.2. Materials

Primers for *GAPDH*, *CAPZB*, *FLNA*, and *CD2AP* were designed using the Primer Bank database hosted by Harvard Medical School (Table 1). The normal human hepatocyte cell line (Lx2) and human HCC cell lines (Huh7, HepG2, and Hep3B) were acquired from the American Type Culture Collection (United States). The cells were cultured at 37°C with 5% carbon dioxide. Total RNA was extracted using TRIzol reagent, followed by complementary DNA (cDNA) synthesis using a cDNA synthesis kit from TaKaRa (United States). Quantitative polymerase chain reaction (qPCR) was performed using ChamQ SYBR qPCR Master Mix (Vazyme, China).

Table 1. Gene and primer sequence

Gene name		Primer sequence (5' – 3')
GAPDH	Forward	CATGAGAAGTATGACAACAGCCT
	Reverse	AGTCCTTCCACGATACCAAAGT
FLNA	Forward	GTCACGGGCTAGGTGCTG
	Reverse	GTCCACATCCACCTCTGAGC
CAPZB	Forward	CCCAGCAAATCGAGAAAAACCT
	Reverse	CAAGGGAGGGTCATACTTGTTAC
CD2AP	Forward	GGCATGGGAATGTAGCAAGTC
	Reverse	CCACCAGCCTTCTTCTACCTC

2.2. Construction and validation of a prognostic model based on DRGs

Univariate Cox regression analysis was employed to evaluate the prognostic value of DRGs. The prognostic risk model was developed using the "survival," "survminer," and "glmnet" packages in R software. Regression coefficients and risk scores were then calculated to establish both risk score and clinical factor models. The risk score formula was defined as follows in Equation I.

$$\text{Risk score} = (\text{Coefficient of regression}_1 \times \text{mRNA expression}_1 + \text{coefficient of regression}_2 \times \text{mRNA expression}_2 + \ldots + \text{coefficient of regression}_n \times \text{mRNA expression}_n \quad \text{(I)}$$

The LASSO-Cox regression model for mRNA was validated by the regression coefficients. HCC patients were stratified into low-risk and high-risk groups based on the median risk score. LASSO regression analysis was utilized to refine the selection of DRGs further. The survival prognosis of the two patient subgroups was evaluated using Kaplan-Meier curves. The mean risk scores were calculated from all HCC samples. Patients with HCC were

categorized into high-risk (≥mean) and low-risk (<mean) groups based on these mean risk scores. Survival curves for these subgroups were then plotted. The "survminer" package in R software generated Kaplan-Meier curves, risk line plots, and scatterplots. These visualizations were used to compare risk score variations among patient subtypes with DRGs and to illustrate the relationship between risk levels and patient survival status. Receiver operating characteristic (ROC) curve analysis, including survival curves at 1, 3, and 5 years, was performed using the "survminer" and "timeROC" packages in R software to assess the prognostic power of the risk model. In addition, risk scores and clinical factors were integrated to construct univariate and multivariate Cox regression models, which were used to evaluate the independent prognostic value of risk scores for HCC patients.

2.3. Analysis of the correlation between prognostic and clinical features

Risk scores and clinical data were integrated and analyzed using the chi-square test to examine the correlation between prognostic and clinical features. The chi-square test was employed to investigate the involvement of prognostic characteristics in the development of HCC. Heatmaps displaying DRGs with clinic-specific data were generated. Box plots based on risk scores were created to analyze the variance in clinical factors and the correlation between prognostic and clinical characteristics. Variables such as age, sex, pathologic N, pathologic M, pathological stage, and pathologic T were considered to determine statistical significance across subgroups. Pathologic T, N, and M refer to tumor, node, and metastasis, respectively. In addition, further stratified analyses were performed to assess the prognostic significance of DRG characteristics within subgroups categorized by age (≤65 years vs. >65 years), sex (male vs. female), pathologic stage (stages I – II vs. stages III – IV), tumor grade (low vs. high), pathologic T (stages T1 – T2 vs. stages T3 – T4), and pathologic N (N0 vs. N1–2–3).

2.4. Nomogram establishment based on risk score and clinical variables

Univariate and multivariate Cox regression analyses and additional clinical variables were incorporated to assess whether risk scores possess independent prognostic value in predicting outcomes. Column-line plots were generated to evaluate the predicted likelihood of overall survival (OS). Clinical variables and risk scores were collected, and Cox regression modeling was applied to calculate hazard ratios (HRs) for each variable. The relationships between DRG-based and clinical variables were examined. Column-line plots were constructed using clinical factors and DRG-based risk ratings to evaluate the likelihood of 1-, 3-, and 5-year OS in patients with HCC. Consistency indices and a calibration curve were employed to assess the predictive accuracy of the nomogram.

2.5. Functional enrichment analyses and protein-protein interaction

Gene ontology (GO) and Kyoto Encyclopedia of Genes and Genomes (KEGG) enrichment analyses were employed to investigate differences in gene functions and pathways between subgroups identified by the risk model. Eighteen DRGs were identified between the low- and high-risk groups in the TCGA dataset. To better understand the biological pathways and functions of the identified differentially expressed genes, GO enrichment analysis (molecular function [MF], biological process [BP], and cellular component [CC]) and KEGG pathway analysis were conducted using the "ClusterProfiler," "org.Hs.eg.db," "enrichplot," and "ggplot2" packages of R software. A $p<0.05$ was considered indicative of significant enrichment.

Protein-protein interactions (PPIs) were visualized by submitting differentially expressed DRGs to the STRING database (http://www.string-db.org/). The most significant modules (the top ten highest-rated genes) within the PPI network were selected using the maximal clique centrality algorithm through the "CytoHubba" plugin in the Cytoscape software (version 3.8.0).

2.6. GSEA

To investigate the potential molecular mechanisms distinguishing the low-risk and high-risk groups, GSEA was performed using the "ClusterProfiler," "enrichplot," "ggplot2," and "org.Hs.eg.db" packages of the R software. A $p<0.05$ was considered indicative of significant enrichment. Pathways with the top five highest numbers of molecules in the gene set were selected for mapping.

2.7. The relationship between prognostic signatures and immune checkpoints

Given the significance of ICI immunotherapy, the association between two subgroups of HCC patients, categorized by risk scores and 79 immune checkpoints, was investigated, and the differences in immune checkpoint expression between these subgroups were assessed. Gene expression associated with immune checkpoints was analyzed using the "limma" and "ggpubr" packages in the R software, focusing on the differences between the high-risk and low-risk groups.

2.8. Correlation analysis between genes and immune infiltration

Immune infiltration refers to the distribution and activity of immune cells and related molecules within tumor

tissues, which is crucial for elucidating tumorigenesis, progression, and therapeutic outcomes. To investigate the relationship between DRG expression and immune cell infiltration, we submitted differentially expressed DRGs to the database (https://cistrome.shinyapps.io/timer/) to acquire information regarding the association between genes and immune cells. A higher correlation coefficient (Cor) indicates a stronger relationship between genes and immune cell infiltration.

2.9. Drug sensitivity analysis

Six DRGs were submitted to the Genomics of Drug Sensitivity in Cancer (GDSC) and the Cancer Therapeutics Response Portal (CTRP) through the Gene Set Cancer Analysis (GSCA) website (http://bioinfo.life.hust.edu.cn/GSCA/#/), which facilitated a more in-depth analysis of the relationship between DRG expression and drug sensitivity in HCC.

3. Results

3.1. Construction and validation of a prognostic model based on DRGs

3.1.1. Heatmap of gene expression levels between normal and tumor tissue

Based on |logFC| >0.5 and a FDR threshold of <0.05, 23 known genes were initially screened. Subsequently, the "limma" package in the R software was utilized to identify genes with differential expression. Through this analysis, 18 DRGs, including *SLC7A11*, *PDLIM1*, *GYS1*, *ACTN4*, *NDUFA11*, *NCKAP1*, *FLNB*, *MYH9*, *MYL6*, *LRPPRC*, *SLC3A2*, *FLNA*, *CD2AP*, *RPN1*, *ACTB*, *CAPZB*, *DSTN*, and *TLN1*, were identified. A heatmap was generated using clinical information from HCC patients to display the expression levels of the 18 genes in both normal and tumor tissues. Analysis of the left dendrogram of the heatmap revealed that *SLC7A11*, *CD2AP*, *GYS1*, and *NCKAP1* exhibited high similarity and were minimally expressed in normal tissues. In addition, the relative expression levels of *ACTB* were higher in both normal and tumor tissues. The expression levels of *MYL6* and *RPN1* were upregulated in most tumor tissues. In contrast, *FLNA*, *ACTN4*, *CAPZB*, and *DSTN* were downregulated in some tumor tissues (Figure 1). The heatmap visually represents specific gene expression (the left dendrogram indicates gene clustering, and the color blocks reflect relative gene expression), facilitating further analysis.

3.1.2. Univariate Cox regression and LASSO regression

Univariate Cox regression analysis was employed to assess the prognostic significance of HCC. It was found that only eight genes (*CAPZB*, *RPN1*, *SLC7A11*, *FLNA*, *NCKAP1*, *CD2AP*, *ACTB*, and *ACTN4*) exhibited significant prognostic value (threshold of $p<0.01$, HR > 1) (Figure 2A). LASSO regression analysis was utilized to select the optimal parameter (Lambda) for the model. Cross-validation was performed by selecting one standard error of the Lambda value, resulting in the most optimal

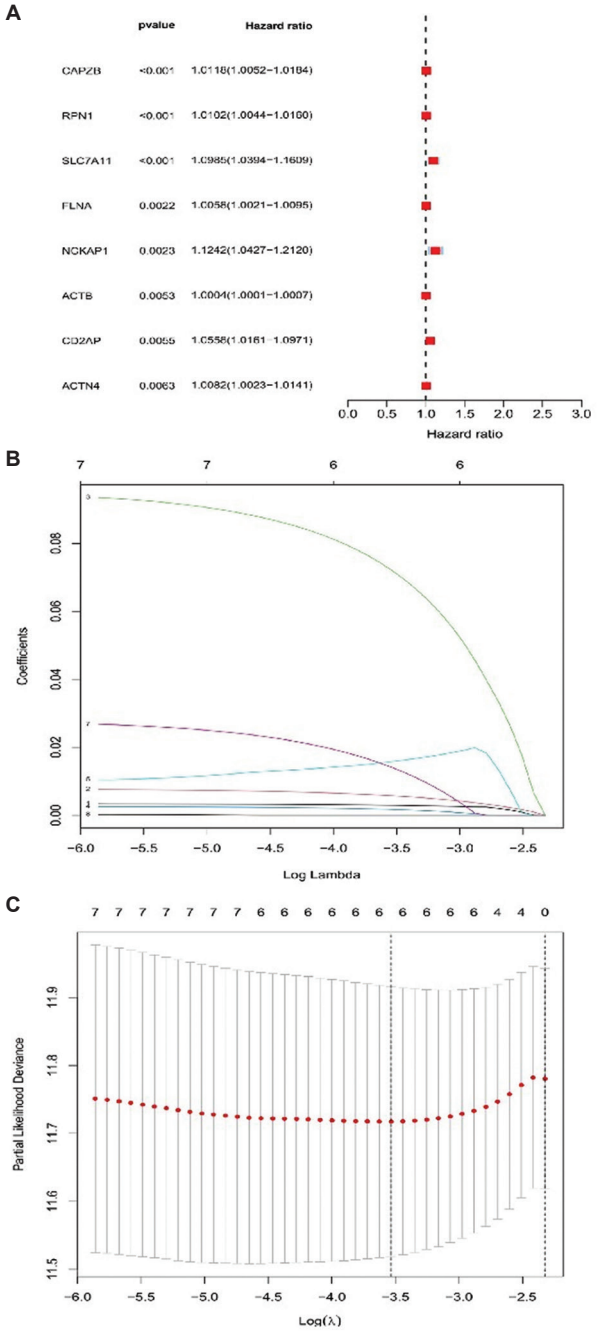


Figure 2. Correlation graphs of univariate Cox regression and LASSO regression. (A) Forest map. (B) LASSO coefficient path diagram. (C) Cross-validation used in the LASSO regression.
Abbreviation: LASSO: Least absolute shrinkage and selection operator.

model value (λ = 0.082469) (Figure 2B and 2C). This process successfully identified six genes (*CAPZB*, *RPN1*, *SLC7A11*, *FLNA*, *NCKAP1*, and *CD2AP*) (Table 2). The six meticulously screened genes underwent regression analysis to compute their respective coefficients and risk scores. Based on the median risk score, these scores were subsequently used to establish a risk model that divided HCC patients into two distinct subgroups: low-risk and high-risk groups. Comparative analysis revealed that the high-risk group, initially comprising 182 individuals, exhibited a significantly lower survival rate than the low-risk group, with 183 patients. Specifically, approximately 140 patients in the low-risk group survived after 1 year, whereas only about 114 patients in the high-risk group survived. Similarly, the survival numbers were 15 and 13, respectively, after 5 years. This stark contrast indicated a statistically significant difference (p<0.001), suggesting a higher mortality rate in the high-risk group (Figure 3A). Consequently, the high-risk group displayed a significantly greater number of deaths and a shorter OS time (Figure 3D). These findings indicated a negative correlation between risk scores and prognosis, implying that a higher risk score is associated with poorer prognosis (Figure 3A-D).

Table 2. Gene list and coefficients

Gene	Coefficients
CAPZB	0.00295
RPN1	0.00575
SLC7A11	0.07195
FLNA	0.00173
NCKAP1	0.01584
CD2AP	0.01404

Time-dependent ROC analysis was performed to assess the prognostic model's reliability. The results showed notable prognostic accuracy, with the area under the curve values of 0.727 for a 1-year prognosis, 0.676 for a 3-year prognosis, and 0.635 for a 5-year prognosis. These findings underscore the model's ability to predict prognosis precisely (Figure 3B). Furthermore, heatmap visualization was used to highlight the differential expression patterns of DRGs between the high-risk and low-risk groups within the TCGA cohort. Notably, six key genes – *CAPZB*, *RPN1*, *SLC7A11*, *FLNA*, *NCKAP1*, and *CD2AP* – exhibited distinct expression profiles. In the high-risk group, these genes showed predominantly elevated expression levels, as

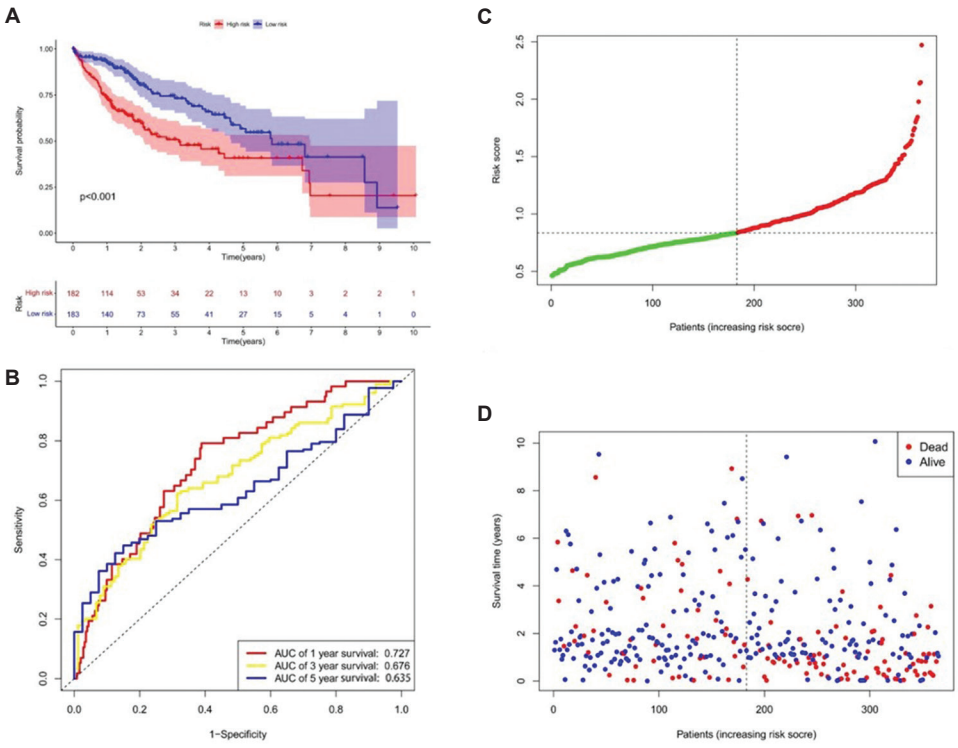


Figure 3. Construction of the prognostic disulfidptosis-related genes-based signature. (A) Kaplan-Meier survival analysis of hepatocellular carcinoma patients between high-risk and low-risk groups (B) Time-independent receiver operating characteristic analysis of risk scores predicting overall survival. (C) Risk line plot (low risk indicated by green and high risk indicated by red. (D) Risk scatterplot.
Abbreviation: AUC: Area under the curve.

indicated by the predominance of red and dark red patches. Conversely, in the low-risk group, their expression was minimal or negligible, as indicated by the predominance of black and dark green patches. This analysis depicts the genetic signatures associated with different risk levels in HCC patients, offering insights into potential therapeutic targets and prognostic biomarkers (Figure S1).

3.1.3. Correlations between the risk score and clinicopathological factors

Univariate Cox regression analysis showed that both the pathologic stage and risk score were significantly associated with the survival of HCC patients (p<0.001) (Figure 4A). Furthermore, multivariate Cox regression analysis indicated a significant association with both the risk score and pathologic stage (p<0.001) (Figure 4B). These findings suggest that DRG-based characterization serves as an independent predictive factor for HCC patients.

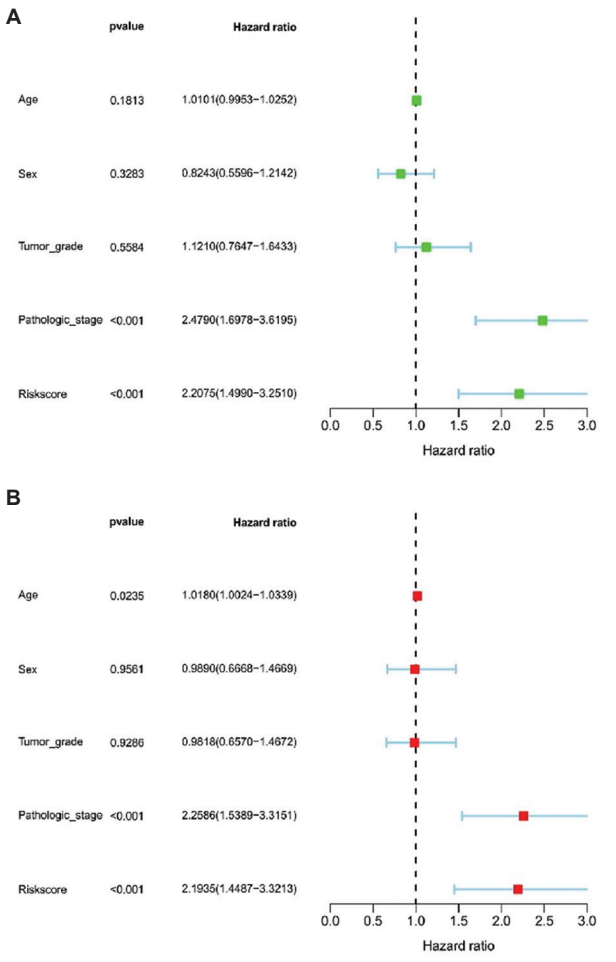


Figure 4. Modeling of risk score correlations with clinical factors. (A) Forest plot for univariate Cox regression analysis. (B) Forest plot for multivariate Cox regression analysis.

Multivariate analysis confirmed that the DRG-based risk score and pathologic stage independently predicted HCC prognosis. While age was included in the model, its association with survival outcomes was not statistically significant, suggesting that the DRG signature and tumor stage are more critical determinants of prognosis in this cohort.

3.2. Correlation between prognostic features and clinical features

3.2.1. Nomogram and calibration curve

The chi-square test was employed to determine whether prognostic characteristics were associated with the development of HCC. The results revealed significant differences between the two subgroups in terms of pathologic stage (p<0.01) and pathologic T (p<0.01). In contrast, no significant differences were observed for age (p=0.171), sex (p=0.153), pathologic N (p=0.413), and pathologic M (p=0.575) (Figures S2 and S3).

In addition, stratified analysis was conducted to assess the prognostic importance of DRGs in both risk groups. The results indicated that DRG-based characteristics were significant predictors for age ≤65 years (p=0.001), age >65 years (p=0.017), female (p=0.017), male (p<0.001), stages I – II of pathologic stage (p<0.001), T1 – T2 stages of pathologic T (p<0.001), N0 of pathologic N (p<0.001), and low tumor grade (p<0.001). However, DRG-based features were less effective in predicting stages III – IV of the pathologic stage (p=0.282), T3 – T4 stages of pathologic T (p=0.234), N1–2–3 of pathologic N (p=1.000), and high tumor grade (p=0.077) (Figure S4).

A nomogram was developed to predict survival in HCC patients further, incorporating tumor grade, pathological stage, risk score, and age to estimate 1-, 3-, and 5-year survival rates (Figure 5A). The calibration curve exhibited minor deviations from the reference gray line, and the consistency indices for the nomogram were 0.9 (1 year), 0.771 (3 years), and 0.662 (5 years), indicating that the actual patient survival closely matched the predicted values (Figure 5B). These results confirm the favorable predictive ability of the nomogram.

3.3. Functional enrichment analyses and PPI

GO and KEGG enrichment analyses were performed to elucidate the potential roles of differentially expressed DRGs. The GO enrichment analysis revealed that 18 DRGs were significantly associated with the regulation of actin filament-based processes, platelet aggregation, homotypic cell-cell adhesion, platelet activation, and blood coagulation. Among these, six DRGs were explicitly

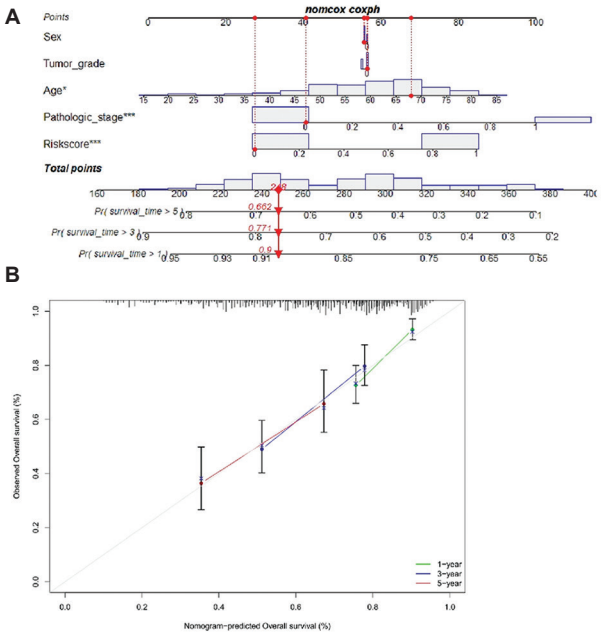


Figure 5. Correlation graphs based on risk scores and clinical variables. (A) Nomogram for predicting 1-, 3-, and 5-year overall survival. (B) The calibration curve for predicting 1-, 3-, and 5-year overall survival.
Note: *Indicates the significance of these two components.

enriched in actin filament-based processes. In addition, 18 DRGs were prominently associated with CCs such as focal adhesion, cell-substrate junction, cell cortex, brush border, and clusters of actin-based cell projections, with eight DRGs being significantly involved in each of these components. Furthermore, the 18 DRGs were notably enriched in MFs related to cadherin binding, actin binding, and actin filament binding, with eight, eight, and seven DRGs involved in each function, respectively (Figure 6A and B).

The KEGG enrichment analysis revealed that 18 DRGs were significantly involved in five metabolic pathways, namely, focal adhesion, motor proteins, tight junction, regulation of actin cytoskeleton, and *Salmonella* infection, with five, four, four, four, and four DRGs associated with each pathway, respectively (Figure 6C and D). The STRING database revealed that the PPI network of differentially expressed DRGs comprised 18 nodes and 37 edges (Figure 7A and B). Using Cytoscape software, the most important modules of the PPI network were identified, with the top 10 highest-scoring genes (*ACTN4*, *ACTB*, *CD2AP*, *CAPZB*, *DSTN*, *FLNA*, *FLNB*, *MYL6*, *MYH9*, and *TLN1*) selected (Figure 7C). The genes identified through

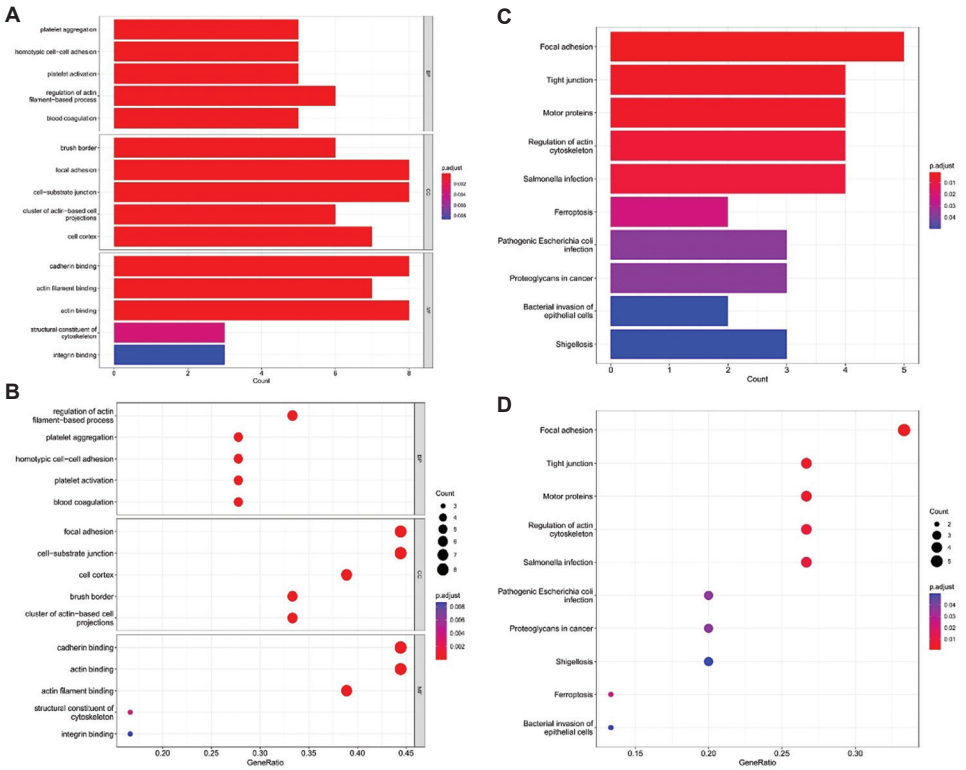


Figure 6. Enrichment analyses of disulfidptosis-related genes. (A) Gene ontology (GO) bar chart. (B) GO bubble chart (each function shows the top five pathway gene sets mainly enriched separately). (C) Kyoto Encyclopedia of Genes and Genomes (KEGG) bar chart. (D) KEGG bubble chart.

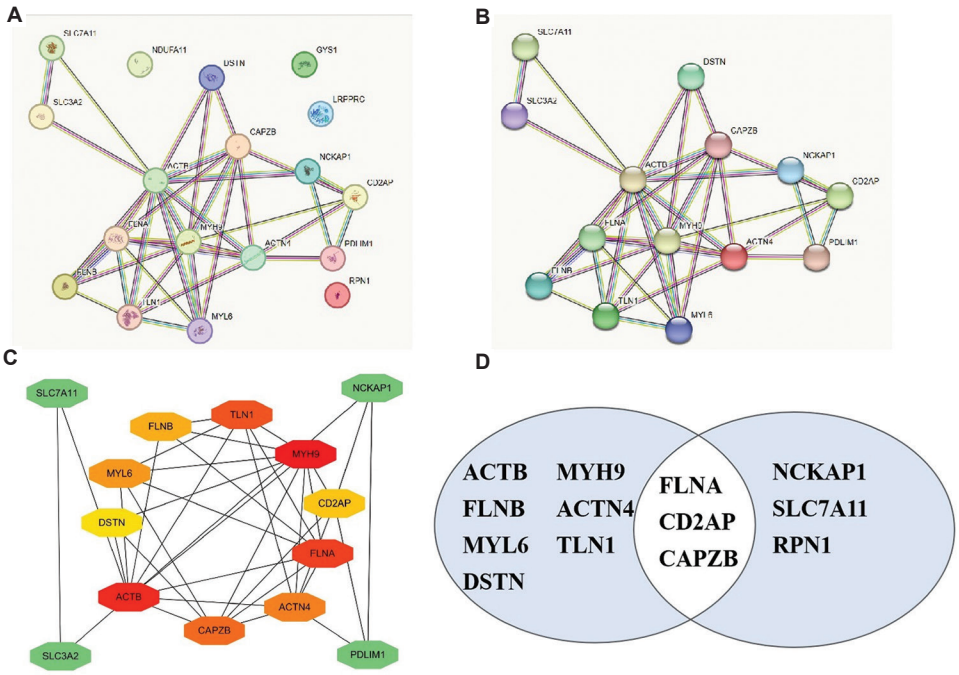


Figure 7. Diagram of the protein-protein interaction network of differentially expressed genes and diagram of the gene network. (A) Network diagram of all genes. (B) Network diagram of genes with edge and node relationships. (C) Gene network map by Cystoscope software. (D) Gene intersection map (*FLNA* and *CAPZB* have been reported to be associated with hepatocellular carcinoma, whereas no detailed hepatocellular carcinoma-related reports have been reported for the *CD2AP* gene).

this approach were compared with the risk model, and it was found that three genes (*FLNA*, *CD2AP*, and *CAPZB*) were common among the 10 genes identified through the gene network analysis, which were further refined by the six critical genes selected through regression analysis (Figure 7D). In addition, this investigation revealed that among the existing research articles related to HCC, *FLNA* and *CAPZB* have been identified as therapeutic markers and are involved in relevant pathways, while *CD2AP* has not been extensively studied in the context of HCC pathways and clinical treatment.

3.4. GSEA

The GSEA analysis was conducted to elucidate the molecular pathways underlying the characterization of DRGs. The GSEA plot results demonstrated that the enrichment scores (enrichment score value: maximum peak) were positive, indicating that the gene sets were enriched at the top of the list (Figure S5). These positive enrichment scores suggest that the DRGs were elevated in the high-risk group, with significant increases observed in efferocytosis, hepatitis C, herpes simplex virus 1 infection, oocyte meiosis, and transcriptional misregulation in cancer. The most significant effects were observed in efferocytosis and oocyte meiosis, with a corrected p=0.0096 (Table 3).

Table 3. Enrichment scores and signal pathways

Description	Set size	Enrichment score	Adjusted p-value
Herpes simplex virus 1 infection	498	0.3849	0.0380
Transcriptional misregulation in cancer	173	0.4245	0.0400
Efferocytosis	149	0.4529	0.0119
Hepatitis C	149	0.4437	0.0260
Oocyte meiosis	127	0.4689	0.0105
Taste transduction	83	0.4902	0.0107
B cell receptor signaling pathway	81	0.4875	0.0260
Acute myeloid leukemia	67	0.4902	0.0312
Cytosolic DNA-sensing pathway	64	0.5040	0.0219
N-Glycan biosynthesis	53	0.5001	0.0433
Aminoacyl-tRNA biosynthesis	25	0.5809	0.0324

3.5. Immune cell infiltration analysis

Differences in immune cell infiltration between risk groups were analyzed using immune cell infiltration analyses of the high- and low-risk groups. The results from Tumor Immune Microenvironment, CIBERSORT, CIBERSORT-ABS, quanTIseq, and Microenvironment Cell Populations-counter computational algorithms revealed that, compared to the low-risk group, the high-risk group exhibited higher

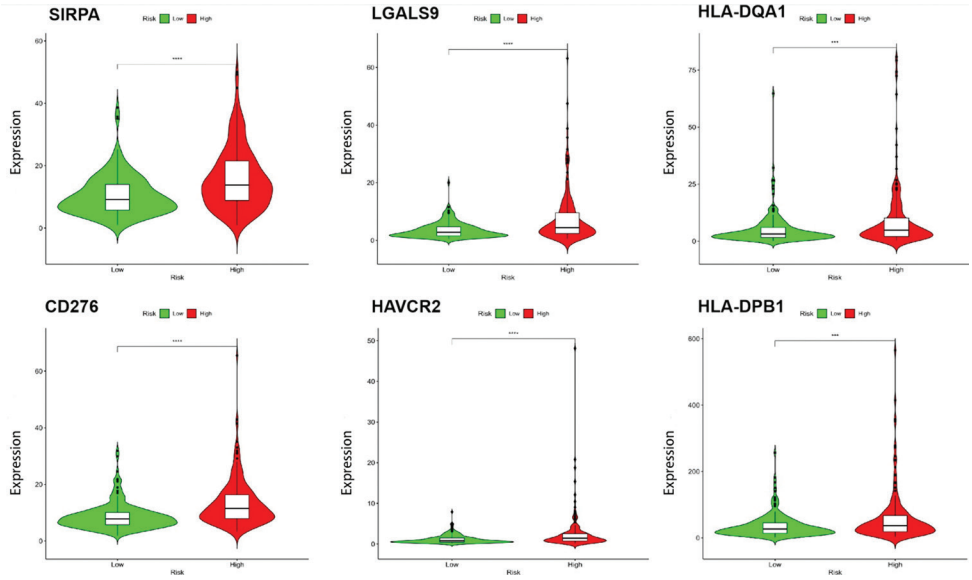


Figure 8. Violin plots indicate the relationship between prognostic signatures and immune checkpoints
Note: Statistical significance was determined at ***p<0.001 and ****p<0.0001.

levels of B cells, CD4⁺ T cells, neutrophils, macrophages, and dendritic cells. In contrast, the Estimating the Proportions of Immune and Cancer Cells algorithm showed no significant differences in immune cell levels between the high- and low-risk groups. This finding suggests that immune-related genes were more abundant in the high-risk group, exhibiting a poorer immune state (Figure S6).

3.6. The relationship between prognostic signatures and immune checkpoints

Based on risk scores, associations with 79 immunological checkpoints were investigated in two patient subgroups with HCC, and the expression of immune checkpoints between these subgroups was examined to determine whether significant differences existed. Given the importance of checkpoint inhibitor immunotherapy, the relationship between risk scores and 79 immune checkpoints was explored, with a focus on six specific checkpoints: *SIRPA*, *LGALS9*, *HLA-DQA1*, *CD276*, *HAVCR2*, and *HLA-DPB1*. The results demonstrated that all six immune checkpoint genes exhibited significantly higher expression in the high-risk group compared to the low-risk group (Figure 8). This elevation suggests the presence of immunosuppressive and exhausted phenotypes in the high-risk patient cohort.

The findings indicated that the six DRGs were most strongly associated with macrophages, neutrophils, CD4⁺ T cells, and dendritic cells (Table 4).

3.7. Drug sensitivity analysis

The results indicated relevance between the expression of six genes and the susceptibility of pan-cancer patients to the top 30 CTRP drugs. Most of these top 30 CTRP drugs exhibited positive correlations with the mRNA expression of the overexpressed genes *FLNA*, *SLC7A11*, and *NCKAP1*. Conversely, the *CD2AP* gene was negatively correlated with bosutinib, lapatinib, and austocystin D, which might enhance the sensitivity of these drugs. In addition, the overexpression of *CD2AP*, *RPN1*, and *CAPZB* genes was observed to increase sensitivity to austocystin D (Figure 9A).

In pan-cancer, relevance was identified between the expression of six genes and sensitivity to the top 30 GDSC drugs, with these highly expressed genes generally showing negative or no association with most of the drugs. The upregulation of *FLNA* was observed to lead to resistance to the small molecule drug WZ3105 while increasing sensitivity to the PI3K p110β inhibitor TGX221, midostaurin, and the HSP90 inhibitor, 17-AAG. The overexpression of *CAPZB* led to resistance to afatinib while increasing sensitivity to pazopanib and dasatinib.

Table 4. The correlation of gene and immune cells

Gene	Immune cell (Correlation coefficients: largest to smallest)		
CAPZB	Macrophage	Dendritic cell	Neutrophil
RPN1	Macrophage	CD4⁺T cell	Neutrophil
SLC7A11	Neutrophil	Dendritic cell	Macrophage
FLNA	CD4⁺T cell	Macrophage	Dendritic cell
NCKAP1	Neutrophil	Macrophage	CD4⁺T Cell
CD2AP	Macrophage	Neutrophil	CD4⁺T Cell

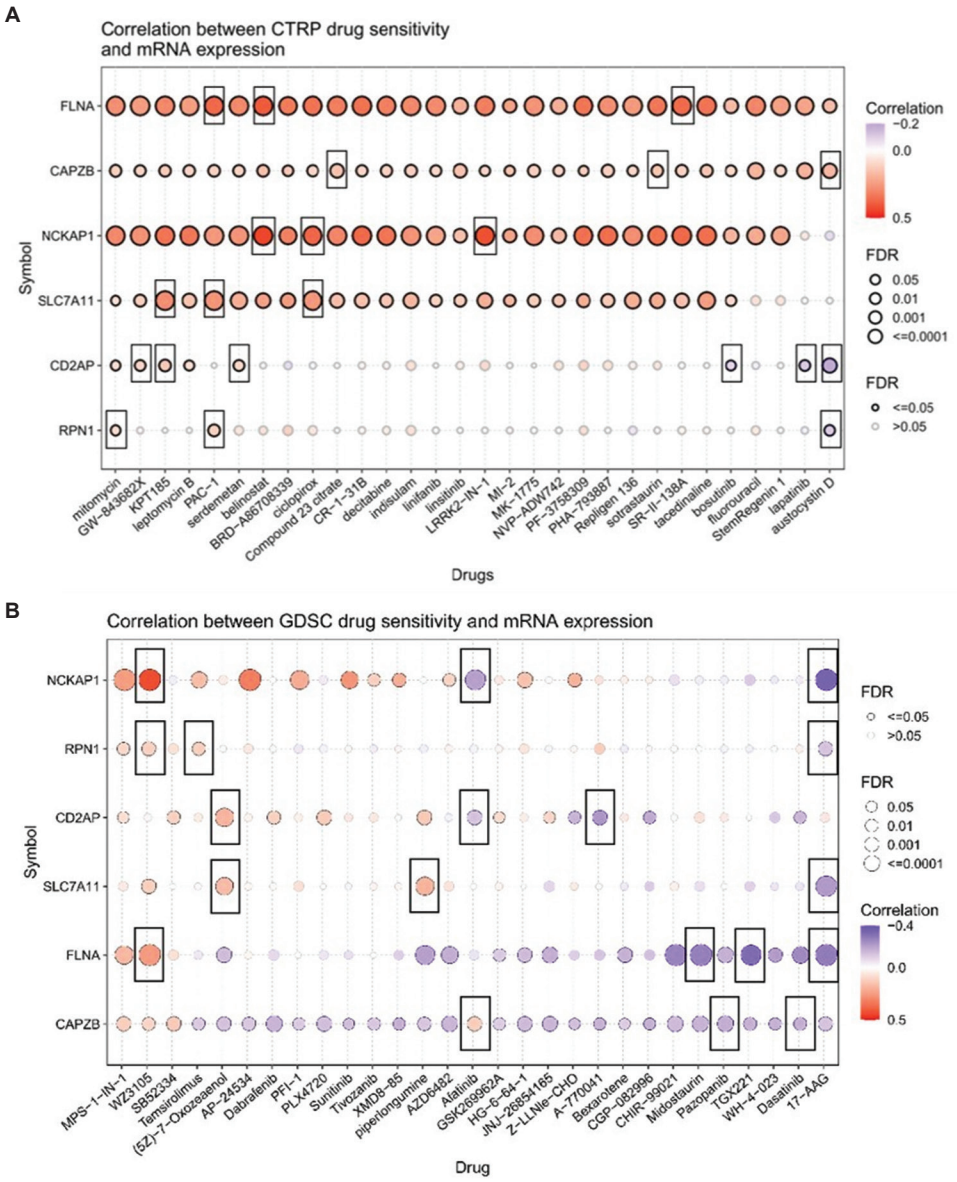


Figure 9. Correlation between six genes and the sensitivity of two database drugs in pan-cancer. (A) Cancer Therapeutics Response Portal (CTRP) drugs. (B) Genomics of Drug Sensitivity in Cancer (GDSC) drugs. The color of the bubble represents the correlation between mRNA expression and inhibitory concentration$_{50}$, and the size of the bubble is positively correlated with a false discovery rate (FDR) significance. The black outline of the bubble indicates an FDR value of <0.05. A positive correlation indicates a higher gene expression may lead to drug resistance, while a negative correlation indicates a higher gene expression may make drugs more sensitive.

In addition, the overexpression of *CD2AP* was observed to lead to resistance to the transforming growth factor-β-activated kinase 1-selective inhibitor, (5Z)-7-Oxozeaenol, while increasing sensitivity to afatinib, and the lymphocyte-specific kinase inhibitor, A-770041. Data patterns evolve, as shown in subsequent analyses (Table 5 and Figure 9B).

In summary, in the CTRP database, CD2AP, RPN1, and CAPZB overexpression increased sensitivity to sanguinarine (austocystin D). In the GDSC database, the upregulated expression of four genes (*RPN1*, *SLC7A11*, *FLNA*, and *NCKAP1*) increased sensitivity to the HSP90 inhibitor, 17-AAG. In addition, the upregulation of *RPN1*, *FLNA*, and *NCKAP1* was observed to result in resistance to the small molecule drug WZ3105. These findings may support drug-targeted therapeutic options for HCC.

3.8. Gene expression levels *in vitro*

According to the results, the expression levels of three common genes (*CAPZB*, *CD2AP*, and *FLNA*) related to

Table 5. Detailed information on the correlation between six genes and sensitivity to drugs from the databases

Gene	Drug	Correlation coefficient	False discovery rate	Correlation
CAPZB	Austocystin D	−0.141087274	0.005804727	Sensitive
	Pazopanib	−0.173849265	0.000033753	Sensitive
	Dasatinib	−0.168540986	0.005699669	Sensitive
	Compound 23 citrate	0.170831678	0.001937341	Resistance
	Sotrastaurin	0.158002623	0.000105721	Resistance
	Afatinib	0.123033433	0.0005555	Resistance
CD2AP	Austocystin D	−0.182505765	0.000015875	Sensitive
	Lapatinib	−0.110737669	0.009629998	Sensitive
	Bosutinib	−0.088728967	0.030302568	Sensitive
	Afatinib	−0.123312839	0.000537566	Sensitive
	A-770041	−0.226790986	0.000493374	Sensitive
	Kpt185	0.231873116	1.94179e-08	Resistance
	Serdemetan	0.222105917	0.168597659	Resistance
	Gw-843682x	0.217489267	2.2246e-08	Resistance
	(5z)-7-oxozeaenol	0.186845876	2.26467e-07	Resistance
FLNA	Tg×221	−0.323452482	4.56928e-09	Sensitive
	Midostaurin	−0.275955206	1.04e-13	Sensitive
	17-AAG	−0.284633046	5.11983e-16	Sensitive
	Belinostat	0.401546268	7.8603e-15	Resistance
	Pac-1	0.371434058	1.68066e-23	Resistance
	Sr-ii-138a	0.36983117	8.11047e-26	Resistance
	Wz3105	0.254281786	5.887e-14	Resistance
NCKAP1	17-AAG	−0.344806738	1.00425e-23	Sensitive
	Afatinib	−0.201855734	4.40804E-09	Sensitive
	Belinostat	0.445100924	2.73907e-18	Resistance
	Lrrk2-in-1	0.422728526	2.33952e-23	Resistance
	Ciclopirox	0.378017857	1.90393e-26	Resistance
	Wz3105	0.431735223	0	Resistance
RPN1	Austocystin D	−0.109550994	0.014444287	Sensitive
	17-AAG	−0.121562945	0.000916013	Sensitive
	Pac-1	0.120091648	0.002415796	Resistance
	Mitomycin	0.090786827	0.019872194	Resistance
	Wz3105	0.114202068	0.001178826	Resistance
	Temsirolimus	0.120785064	0.003797259	Resistance
SLC7A11	17-AAG	−0.217447834	1.08873e-09	Sensitive
	Kpt185	0.286751228	2.40003e-11	Resistance
	Pac-1	0.270432867	1.06578e-12	Resistance
	Ciclopirox	0.260975547	7.26742e-13	Resistance
	(5z)-7-oxozeaenol	0.175243229	1.40465e-06	Resistance
	Piperlongumine	0.189664289	3.33815e-07	Resistance

DGRs and immune checkpoints in HCC cell lines were further investigated *in vitro*. The results showed that the mRNA expression levels of *CAPZB* and *CD2AP* were higher in Huh7 and Hep3B cells than in normal hepatocyte cells, and no significant difference was observed in HepG2 cells. The mRNA expression levels of *FLNA* in the three HCC

cell lines were significantly lower than those in normal hepatocyte cells (Figure 10).

4. Discussion

In recent years, the incidence of liver cancer has been on the rise,[20] with HCC constituting the majority of liver cancer diagnoses and deaths.[21] Recent studies have identified a novel form of cell death termed disulfidptosis,[8] which demonstrates functional relevance in certain malignancies.[8,22] In HCC, where chronic hepatitis B virus infection constitutes the predominant risk factor, Zhang *et al.*[23] successfully constructed a prognostic model comprising five signature genes through systematic analysis of tumor prognostic characteristics associated with disulfidptosis and differential expression patterns of DRGs. The model demonstrates robust efficacy in predicting overall patient survival outcomes. Furthermore, the investigators evaluated the therapeutic implications of these signature genes across distinct risk subgroups, revealing that all five genes contribute significantly to tumor progression. Quantitative expression profiling of these genes enabled precise stratification of patients into molecular subtypes with differential prognostic trajectories. These findings collectively suggest the feasibility of targeting DRGs as a viable immunotherapeutic strategy.

This study developed a model based on the risk scores of DRGs and clinical factors in HCC. The functions and relationships of DRGs in prognosis prediction, immune infiltration, and immune checkpoints in HCC were elucidated. These findings provide a framework for predicting clinical prognosis, immune infiltration, and responses to immunotherapy, offering novel concepts and methods for targeting immunotherapy and managing patients. Six key genes (*CAPZB*, *RPN1*, *SLC7A11*, *FLNA*, *NCKAP1*, and *CD2AP*) were identified through risk modeling, and the model's strong predictive ability was confirmed by the ROC curves. Functional analysis revealed that the DRGs in the low-risk and high-risk groups correlated with several actin-related pathways,

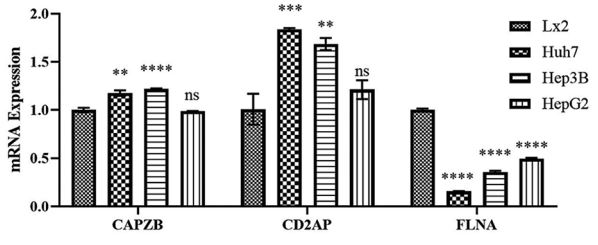


Figure 10. Expression of disulfidptosis-related genes in liver cancer cell lines

Notes: Statistical significance determined at **p*<0.01, ****p*<0.001, and *****p*<0.0001); ns indicates no significance.

with the regulation of the action network being one of the identified mechanisms of disulfidptosis.[8,13,16] Compared to the low-risk group, immune infiltrating cells were generally more prevalent in the high-risk group and were positively correlated with most immune cell types. Ten key genes were identified through gene network analysis and were compared with the risk model, with three genes (*FLNA*, *CD2AP*, and *CAPZB*) being common in both. *FLNA* and *CAPZB* have been reported to be associated with therapeutic markers of HCC. In contrast, no precise studies have been conducted on the *CD2AP* gene concerning HCC pathways or clinical treatment.

Each of these three genes has distinct functions and plays a significant role in disease research. *FLNA* has been investigated as a potential marker for HCC[24,25] and has been shown to interact with other proteins to inhibit the progression of HCC. *CAPZB* has been demonstrated in a single study to be associated with invasion and metastasis in HCC.[26] Similarly, *CD2AP* has been extensively studied in other cancers, but no published studies have reported its direct role in HCC. *FLNA* is a cytoplasmic protein with multiple functions, including interacting with actin-binding proteins to form the cytoskeleton, participating in cell motility, regulating receptor expression, interfering with signaling pathways, and playing a critical role in the development of various tumors.[27] Donadon *et al.*[28] reported that *FLNA* was expressed exclusively in HCC and not in normal liver tissue.[28] In 2021, Sheng *et al.*[29] confirmed that *FLNA* is highly expressed in HCC tissues compared to adjacent non-tumor tissues and is associated with early recurrence following resection surgery.[29] Moreover, Li *et al.*[27] reported that semaphorin 3d can regulate the invasion and metastasis of HCC cells by interacting with *FLNA*, influencing cytoskeletal remodeling, and inhibiting the PI3K/Akt signaling pathway.[27]

CD2-associated protein (CD2AP) encodes a scaffolding molecule that regulates the actin cytoskeleton. This gene has been extensively studied in other cancers, but comprehensive research on its relationship with HCC is lacking. For example, in 2016, Ren and Sheng[30] demonstrated that *CD2AP* is involved in the PI3K/Akt signaling pathway, which is implicated in cellular processes such as metabolism, proliferation, differentiation, and apoptosis.[30] In 2020, Xie *et al.*[31] found that *CD2AP* expression levels were significantly lower in diffuse gastric cancer tissues, which were associated with poor prognosis. Inhibition of *CD2AP* promoted intercellular adhesion and affected the cytoskeleton by interacting with CAPZA1, enhancing cell migration and invasion. In contrast, overexpression of *CD2AP* could attenuate metastasis in gastric cancer. Therefore, *CD2AP* may serve as a novel

biomarker associated with favorable prognosis in gastric cancer patients.[31] Chen *et al.*[32] reported that *CD2AP* can be used as a diagnostic and prognostic biomarker in patients with clear cell renal carcinoma and that DNA hypermethylation plays a significant role in reducing *CD2AP* expression.[32] In addition, *CD2AP* was upregulated in response to chronic hepatitis C virus infection, which stimulates viral transmission and steatosis by disrupting insulin signaling. Targeting *CD2AP* may offer a strategy to alleviate hepatitis C virus infection and its associated liver pathology.[33]

Therefore, *CAPZB*, *FLNA*, and *CD2AP* are anticipated to serve as novel molecular targets and offer valuable tools for assessing the effects of immunotherapy. However, this study has several limitations. For instance, data sourced from public databases were used for bioinformatics analysis, and the prediction results may be biased due to variations among different databases. Additional studies are required to validate the prediction results. In addition, the precise mechanism of *CD2A*P in HCC requires further investigation.

5. Conclusion

This study identified that DRGs are associated with the prognosis and immune status of patients with HCC. Three key genes (*CAPZB*, *FLNA*, and *CD2AP*) are crucial for further elucidating the role of DRGs in HCC. In addition, targeting differentially expressed genes may offer new approaches for diagnosing and treating HCC. Furthermore, *CD2AP* has not yet been reported to be associated with HCC pathways and clinical treatment. Hence, it may serve as a novel tumor marker and offer a potential therapeutic strategy for HCC.

Acknowledgments

None.

Funding

None.

Conflict of interest

The authors declare they have no competing interests.

Author contributions

Conceptualization: Shanshan Wang
Investigation: Yang Li
Methodology: Xin Xie
Formal analysis: Moxian Chen
Writing – original draft: Qiang Li
Writing – review & editing: Jiaqian Mo

Ethics approval and consent to participate

Not applicable.

Consent for publication

Not applicable.

Availability of data

Publicly available datasets were analyzed in this study. Clinical data for 424 patients with HCC were obtained from the TCGA database (https://portal.gdc.cancer.gov/).

References

1. Bray F, Laversanne M, Sung H, *et al.* Global cancer statistics 2022: GLOBOCAN estimates of incidence and mortality worldwide for 36 cancers in 185 countries. *CA Cancer J Clin*. 2024;74(3):229-263.

   doi: 10.3322/caac.21834

2. Sung H, Ferlay J, Siegel RL, *et al.* Global cancer statistics 2020: GLOBOCAN estimates of incidence and mortality worldwide for 36 cancers in 185 countries. *CA Cancer J Clin*. 2021;71(3):209-249.

   doi: 10.3322/caac.21660

3. Zheng RS, Chen R, Han BF, *et al.* Cancer incidence and mortality in China, 2022. *Zhonghua Zhong Liu Za Zhi*. 2024;46(3):221-231.

   doi: 10.3760/cma.j.cn112152-20240119-00035

4. Yang JD, Hainaut P, Gores GJ, Amadou A, Plymoth A, Roberts LR. A global view of hepatocellular carcinoma: Trends, risk, prevention and management. *Nat Rev Gastroenterol Hepatol*. 2019;16(10):589-604.

   doi: 10.1038/s41575-019-0186-y

5. Villanueva A. Hepatocellular carcinoma. *N Engl J Med*. 2019;380(15):1450-1462.

   doi: 10.1056/NEJMra1713263

6. Sangro B, Sarobe P, Hervás-Stubbs S, Melero I. Advances in immunotherapy for hepatocellular carcinoma. *Nat Rev Gastroenterol Hepatol*. 2021;18(8):525-543.

   doi: 10.1038/s41575-021-00438-0

7. Llovet JM, Castet F, Heikenwalder M, *et al.* Immunotherapies for hepatocellular carcinoma. *Nat Rev Clin Oncol*. 2022;19(3):151-172.

   doi: 10.1038/s41571-021-00573-2

8. Liu X, Nie L, Zhang Y, *et al.* Actin cytoskeleton vulnerability to disulfide stress mediates disulfidptosis. *Nat Cell Biol*. 2023;25(3):404-414.

   doi: 10.1038/s41556-023-01091-2

9. Wang Z, Du X, Lian W, *et al.* A novel disulfidptosis-

associated expression pattern in breast cancer based on machine learning. *Front Genet*. 2023;14:1193944.

doi: 10.3389/fgene.2023.1193944

10. Li M, Wang J, Zhao Y, *et al.* Identifying and evaluating a disulfidptosis-related gene signature to predict prognosis in colorectal adenocarcinoma patients. *Front Immunol*. 2024;15:1344637.

doi: 10.3389/fimmu.2024.1344637

11. Li XM, Liu SP, Li Y, Cai XM, Zhang SB, Xie ZF. Identification of disulfidptosis-related genes with immune infiltration in hepatocellular carcinoma. *Heliyon*. 2023;9(8):e18436.

doi: 10.1016/j.heliyon.2023.e18436

12. Wada F, Koga H, Akiba J, *et al.* High expression of CD44v9 and xCT in chemoresistant hepatocellular carcinoma: Potential targets by sulfasalazine. *Cancer Sci*. 2018;109(9):2801-2810.

doi: 10.1111/cas.13728

13. Koppula P, Zhuang L, Gan B. Cystine transporter SLC7A11/xCT in cancer: Ferroptosis, nutrient dependency, and cancer therapy. *Protein Cell*. 2021;12(8):599-620.

doi: 10.1007/s13238-020-00789-5

14. Zhu JH, De Mello RA, Yan QL, *et al.* MiR-139-5p/SLC7A11 inhibits the proliferation, invasion and metastasis of pancreatic carcinoma via PI3K/Akt signaling pathway. *Biochim Biophys Acta Mol Basis Dis*. 2020;1866(6):165747.

doi: 10.1016/j.bbadis.2020.165747

15. Machesky LM. Deadly actin collapse by disulfidptosis. *Nat Cell Biol*. 2023;25(3):375-376.

doi: 10.1038/s41556-023-01100-4

16. Zheng P, Zhou C, Ding Y, Duan S. Disulfidptosis: A new target for metabolic cancer therapy. *J Exp Clin Cancer Res*. 2023;42(1):103.

doi: 10.1186/s13046-023-02675-4

17. Ji PY, Li ZY, Wang H, Dong JT, Li XJ, Yi HL. Arsenic and sulfur dioxide co-exposure induce renal injury via activation of the NF-κB and caspase signaling pathway. *Chemosphere*. 2019;224:280-288.

doi: 10.1016/j.chemosphere.2019.02.111

18. Oduro PK, Zheng X, Wei J, *et al.* The cGAS-STING signaling in cardiovascular and metabolic diseases: Future novel target option for pharmacotherapy. *Acta Pharm Sin B*. 2022;12(1):50-75.

doi: 10.1016/j.apsb.2021.05.011

19. Hu FF, Liu CJ, Liu LL, Zhang Q, Guo AY. Expression profile of immune checkpoint genes and their roles in predicting immunotherapy response. *Brief Bioinform*. 2021;22(3):bbaa176.

doi: 10.1093/bib/bbaa176

20. Siegel RL, Miller KD, Fuchs HE, Jemal A. Cancer statistics, 2022. *CA Cancer J Clin*. 2022;72(1):7-33.

doi: 10.3322/caac.21708

21. Tang Y, Zhang Y, Hu X. Identification of potential hub genes related to diagnosis and prognosis of hepatitis B virus-related hepatocellular carcinoma via integrated bioinformatics analysis. *Biomed Res Int*. 2020;2020:4251761.

doi: 10.1155/2020/4251761

22. Xu K, Zhang Y, Yan Z, *et al.* Identification of disulfidptosis related subtypes, characterization of tumor microenvironment infiltration, and development of DRG prognostic prediction model in RCC, in which MSH3 is a key gene during disulfidptosis. *Front Immunol*. 2023;14:1205250.

doi: 10.3389/fimmu.2023.1205250

23. Zhang C, Zhang X, Dai S, Yang W. Exploring prognosis and therapeutic strategies for HBV-HCC patients based on disulfidptosis-related genes. *Front Genet*. 2024;15:1522484.

doi: 10.3389/fgene.2024.1522484

24. Ai J, Huang H, Lv X, *et al.* FLNA and PGK1 are two potential markers for progression in hepatocellular carcinoma. *Cell Physiol Biochem*. 2011;27(3-4):207-216.

doi: 10.1159/000327946

25. Patarat R, Riku S, Kunadirek P, *et al.* The expression of FLNA and CLU in PBMCs as a novel screening marker for hepatocellular carcinoma. *Sci Rep.* 2021;11(1):14838.

doi: 10.1038/s41598-021-94330-1

26. Li W, Li M, Liao D, *et al.* Carboxyl-terminal truncated HBx contributes to invasion and metastasis via deregulating metastasis suppressors in hepatocellular carcinoma. *Oncotarget*. 2016;7(34):55110-55127.

doi: 10.18632/oncotarget.10399

27. Li Y, Xu C, Sun B, Zhong F, Cao M, Yang L. Sema3d restrained hepatocellular carcinoma progression through inactivating Pi3k/Akt signaling via interaction with FLNA. *Front Oncol*. 2022;12:913498.

doi: 10.3389/fonc.2022.913498

28. Donadon M, Di Tommaso L, Soldani C, *et al.* Filamin a expression predicts early recurrence of hepatocellular carcinoma after hepatectomy. *Liver Int*. 2018;38(2):303-311.

doi: 10.1111/liv.13522

29. Sheng F, Chen KX, Liu J, *et al.* Chromium (VI) promotes EMT by regulating FLNA in BLCA. *Environ Toxicol*. 2021;36(8):1694-1701.

doi: 10.1002/tox.23165

30. Ren Q, You Yu S. CD2-associated protein participates in podocyte apoptosis via PI3K/Akt signaling pathway. *J Recept Signal Transduct Res*. 2016;36(3):288-291.

doi: 10.3109/10799893.2015.1101137

31. Xie W, Chen C, Han Z, *et al.* CD2AP inhibits metastasis in gastric cancer by promoting cellular adhesion and cytoskeleton assembly. *Mol Carcinog*. 2020;59(4):339-352.

doi: 10.1002/mc.23158

32. Chen C, Xu J, Zhang JX, *et al.* CD2AP is a potential prognostic biomarker of renal clear cell carcinoma. *Cancer Med*. 2024;13(4):e7055.

doi: 10.1002/cam4.7055

33. Zhang H, Zhang C, Tang H, *et al.* CD2-associated protein contributes to hepatitis C, virus propagation and steatosis by disrupting insulin signaling. *Hepatology*. 2018;68(5):1710-1725.

doi: 10.1002/hep.30073